Species Richness and Speciation Rates for all Terrestrial Animals Emerge from a Synthesis of Ecological Theories

LUCAS D. FERNANDES[1], ROGIER E. HINTZEN[1], SAMUEL E. D. THOMPSON[1],
TATSIANA BARYCHKA[2], DEREK TITTENSOR[3,4], MICHAEL HARFOOT[4,5], TIM NEWBOLD[2],
AND JAMES ROSINDELL[1,*]

[1]*Department of Life Sciences, Imperial College London, Silwood Park, Buckhurst Road, Ascot, Berkshire, SL5 7PY, UK*
[2]*Centre for Biodiversity and Environment Research, Department of Genetics, Evolution and Environment, University College London,
Gower Street, London, WC1E 6BT, UK*
[3]*Department of Biology, Life Science Centre, Dalhousie University, 6287 Alumni Cres, PO BOX 15000, Halifax, NS, B3H 4R2, Canada*
[4]*United Nations Environment Programme World Conservation Monitoring Centre, 219 Huntingdon Rd, Cambridge CB3 0DL, UK*
[5]*Vizzuality, Calle de Fuencarral 123 8B, Madrid 28010, Spain*
**Correspondence to be sent to: Department of Life Sciences, Imperial College London, Silwood Park, Buckhurst Road, Ascot, Berkshire,
SL5 7PY, UK, E-mail: j.rosindell@imperial.ac.uk.*

Abstract.—The total number of species on earth and the rate at which new species are created are fundamental questions for ecology, evolution and conservation. These questions have typically been approached separately, despite their obvious interconnection. In this study, we approach both questions in conjunction, for all terrestrial animals. To do this, we combine two previously unconnected bodies of theory: general ecosystem models and individual-based ecological neutral theory. General ecosystem models provide us with estimated numbers of individual organisms, separated by functional group and body size. Neutral theory, applied within a guild of functionally similar individuals, connects species richness, speciation rate, and number of individual organisms. In combination, for terrestrial endotherms where species numbers are known, they provide us with estimates for speciation rates as a function of body size and diet class. Extrapolating the same rates to guilds of ectotherms enables us to estimate the species richness of those groups, including yet to be described. We find that speciation rates per species per million years decrease with increasing body size. Rates are also higher for carnivores compared to omnivores or herbivores of the same body size. Our estimate for the total number of terrestrial species of animals is in the range $1.03 - 2.92$ million species, a value consistent with estimates from previous studies, despite having used a fundamentally new approach. Perhaps what is most remarkable about these results is that they have been obtained using only limited data from larger endotherms and their speciation rates, with the predictive process being based on mechanistic theory. This work illustrates the potential of a new approach to classic eco-evolutionary questions, while also adding weight to existing predictions. As we now face an era of dramatic biological change, new methods will be needed to mechanistically model global biodiversity at the species and individual organism level. This will be a huge challenge but the combination of general ecosystem models and neutral theory that we introduce here is a way to tractably achieve it. [Body size; diet; global diversity; general ecosystem model; Madingley model; neutral theory; speciation rate.]

Understanding speciation and how it varies between different groups is central to the interpretation of biodiversity patterns, and to our understanding of the fundamental processes that create biodiversity. Speciation, in turn, is conceptually linked to counts of the species it generates, providing an important gauge for the diversity of life. With planet Earth's current trajectory towards a potential sixth mass extinction event (Barnosky et al. 2011; De Vos et al. 2015; Penn and Deutsch 2022), the ability to estimate global species richness, including the many undescribed species, is all the more relevant to provide a baseline for what we have to lose.

A wide range of methods for estimating speciation rates exists. Many of the current methods use molecular reconstructed phylogenies, complemented with fossil and taxonomic data, and obtain these rates by lineage-based inference (Jetz et al. 2012; Pyron and Burbrink 2013; Rabosky et al. 2014), for an extensive review of these methods, see also (Morlon 2014; Pennell

and Harmon 2013). Although new methodologies have been developed to take into account time, diversity, and trait dependencies on speciation rates (FitzJohn 2010; Pyron and Burbrink 2013; Herrera-Alsina et al. 2019), these approaches are still limited by the availability of data on extinct and extant taxa. Moreover, speciation rates are inextricably connected to extinction rates, and the estimation of the latter is challenging, particularly in cases where there is no fossil data of now extinct species to inform methods (Rabosky 2010). Recent work has also suggested that the inference models for speciation and extinction rates present intrinsic methodological limitations, leading to infinite indistinguishable diversification scenarios of speciation rates for the same time-calibrated phylogenies (Louca and Pennell 2020).

One of the fundamental features of our planet, global species richness, including undescribed species, is a great challenge to estimate. Despite the potential for

a conceptual link to the question of speciation rates, the question of global richness has been approached largely independently. One reason for the difficulty is that limited sampling has precluded direct estimation of the total number of extant species. Indirect estimation of global richness has relied on many approaches, some of which include the opinion of taxonomic experts (Gaston 1991; Stork 1993), inferences based on macroecological patterns (Raven 1985; May 1988; Hawksworth 1991), and trends in taxonomic data accumulation (Mora et al. 2011), with phylogenetic approaches likely to become more important in the future (Billaud et al. 2020). However, the controversy about the underlying assumptions of such approaches (Gaston and Blackburn 2000; Bouchet and Duarte 2006) and the large inherent uncertainty mean that the question of total diversity of species on earth is not fully resolved.

Given the methodological difficulties of estimating speciation rates and patterns of species richness using statistical inference, a promising alternative would be to obtain these estimates via mechanistic models of biological diversity. Indeed, there are many reasons to prefer mechanistic models over statistical inference or correlative models, especially where there is a lack of data (Grimm 1999; Yates et al. 2000). By explicitly representing the underlying processes that affect the biodiversity units of interest, mechanistic models allow the exploration of novel ecological conditions and the generalization of scenarios across data shortfalls (Connolly et al. 2017). Importantly, they also have emergent behavior, making predictions that do not follow trivially from the original model assumptions. Such emergent predictions across multiple dimensions of ecology enable a stronger test of the model's ability to capture underlying processes.

In this study, we combine the benefits of two very different mechanistic approaches: General Ecosystem Models (Harfoot et al. 2014) and Ecological Neutral Theory (Caswell 1976; Hubbell 2011). The Madingley Model is a General Ecosystem Model of global heterotrophic life (Harfoot et al. 2014), that makes predictions of, among other things, the numbers of individual organisms and demographic rates for different functional groups based on fundamental ecological assumptions. Neutral Theory (Hubbell 2011), on the other hand, by ignoring functional differences and focusing primarily on species, provides a tractable approach to connect species richness, speciation rates and number of individual organisms within individual functional groups. The potential synthesis of these approaches could help to relax their individual assumptions, and build a more unified theoretical ecology structure that integrates both functional group and species-focused paradigms. The concept follows previous work based on the idea of nesting neutral models within a niche-based model of some kind (Chisholm and Pacala 2010; Chisholm et al. 2016).

We implement a novel approach, building a pipeline that connects the Madingley and neutral models. The Madingley model allows us to estimate numbers of individual organisms globally for functional groups of terrestrial endotherms and ectotherms. Neutral Theory allows us to connect number of individuals to speciation rates and species richness within any given functional group. By linking these models, we are able to estimate speciation rates for functional groups with known species richness. Conversely, we can estimate species richness for functional groups with given speciation rates. We first apply the pipeline to well-known groups of endotherms based on empirical species richnesses. We then extrapolate these patterns to estimate speciation rates for ectotherms. Finally, we run the pipeline in the other direction to recover the expected species richness of ectotherms, including all undescribed species.

Our aim with this work is to demonstrate a proof of concept for a novel synthesis of mechanistic ecological theories. Then to show their utility as a way to calculate speciation rates and estimate global richness for all terrestrial ectotherms and endotherms.

Materials and Methods

First, we ran the Madingley model, using its default parameter settings (Harfoot et al. 2014), and gathered data from it including total number of individual organisms in each functional group. Next, we developed individual-based "life history" simulations of reproduction, maturation and death to acquire generation lengths of each functional group, based on the Madingley simulations. We gathered empirical data on global species richness of terrestrial endotherms and use it with analytical approximations of a neutral model, and the numbers of individual organisms from the Madingley model, to predict speciation rates per capita per generation for each functional group. We then convert these to rates per species per million years using the generation length data. Finally, we extrapolate these speciation rates for ectotherms and use the neutral model and numbers of individuals from the Madingley model again, but this time to recover species richness. Please refer to Figure 1 for a conceptual overview of the methods.

The choice of dividing biodiversity into endotherms and ectotherms thus comes from the original separation of the groups in the Madingley model, devised to account for the effect of thermoregulation on the ecological processes of interest. In the context of this work, the separation also enables the use data rich endotherms to extrapolate speciation rates for relatively data poor ectotherms.

The Madingley Model

The Madingley model divides global-scale marine and terrestrial environments into 2D grid cells. Each grid cell contains a mixture of individual organisms that
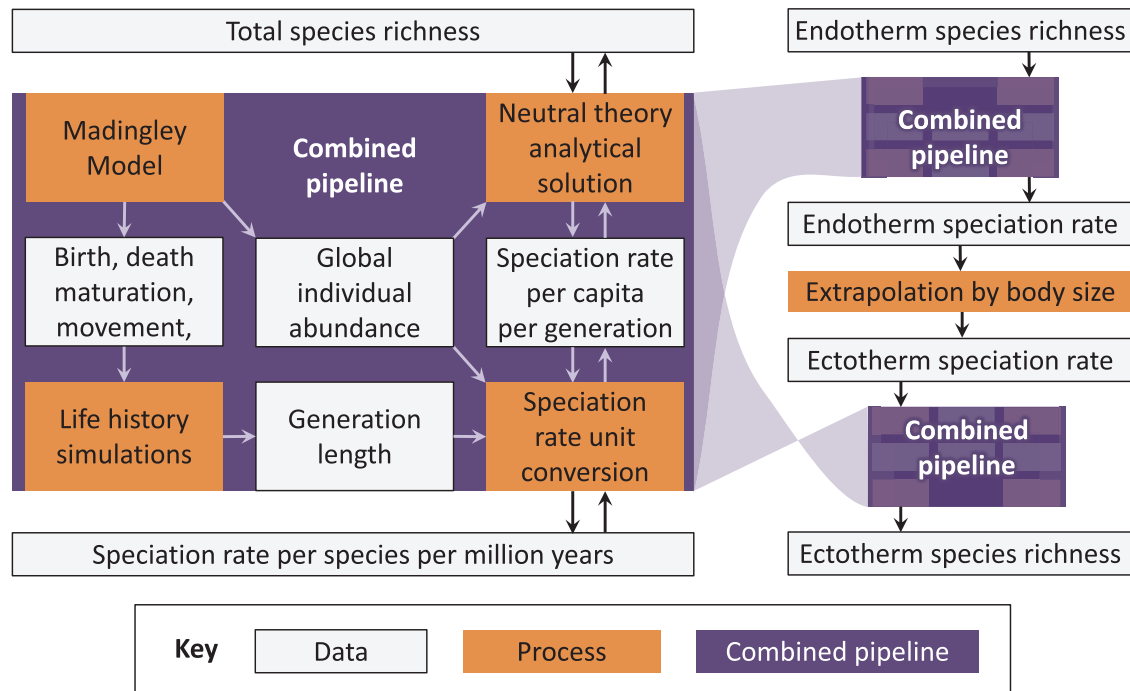
FIGURE 1. Conceptual overview of the methods and analysis pipeline. The dark purple boxes correspond to our main pipeline, which can be run in either direction: to get speciation rate per species per million years from species richness, or vice versa. Lighter orange boxes show processes including simulations and analytical models, off-white boxes show data, including intermediate data products. The left part of the diagram shows the components of our main bi-directional pipeline. The right part of the diagram shows how this pipeline is used in both directions to achieve an estimate of global richness of terrestrial ectotherms. The light transparent shaded regions show how the pipeline exists within each of the blocks on the right part of the diagram, in reverse when used on the second occasion. The full analysis shown in this diagram is repeated for a full range of functional groups (e.g., herbivore, carnivore, and omnivore functional groups in terrestrial endotherms).

may interact in complex ways and disperse to other grid cells (Harfoot et al. 2014). Heterotrophic life is divided into nineteen functional groups that differ in their thermoregulation (endotherm or ectotherm), reproductive strategy (iteroparous or semelparous) and diet class (herbivore, omnivore or carnivore). Further ecological generalizations are used within each of these groups: a continuously varying body mass trait dictates the metabolic scaling, movement and trophic interactions of an organism across distinct juvenile and adult life stages. Ecological interactions are governed by fundamental mechanisms such as size-structured predation (Williams et al. 2010) and type-III Holling functional responses (Holling 1959). Since tracking each individual in a global-scale implementation of the model would be computationally infeasible or arguably even impossible (Purves et al. 2013; Harfoot et al. 2014), identical individual organisms within a given local community are grouped together in "cohorts." Each cohort is described by its categorical functional group and by its continuous body-size trait. All the individuals in the same cohort reproduce, mature, disperse, or die as a group, with either the same process rate or probability of dying applying to all individuals within any given cohort. This kind of approach may be the only way to make a global individual-based mechanistic models tractable (Purves et al. 2013).

Probing the Madingley Model Simulations for Data

It is computationally infeasible to collect data independently on every cohort in the model, due to the sheer size of the system being simulated, which would require too much memory to be stored at every time step of the simulation. To resolve this, we divided endothermic heterotrophic life from the Madingley model into discrete bins based on body mass. Starting from the minimum body mass, for each functional group, successive bin boundaries differ by a factor of 2. Using herbivorous endotherms as an example, the first bin includes masses from 1.5 g to 3.0 g, the second from 3.0 g to 6.0 g, and so on. Thus, pairs of individuals whose body size differs by a factor of more than 2 cannot be in the same bin. This logarithmic binning gives a higher resolution on the small end of the body mass distribution, where most individuals lie, and is more natural for investigating allometric scaling. Narrower body size ranges would have much higher computational cost on what was already a computationally intensive simulation and analysis. The same procedure was conducted separately for each of 3 diet classes of endotherms: herbivore, carnivore, and omnivore; we do not refer to these as trophic levels because all 3 diet classes vary over orders of magnitude in size. Each size bin, within each functional group, is hereafter referred to as a "guild." Whenever a mass value for

a guild is used, it represents the midpoint body mass (in arithmetic space) of the bin in which that guild sits. We collected per capita rates of maturation, death and dispersal between adjacent cells, as well as the number of births and total abundance. These rates were collected separately for each guild, for each month of the annual cycle, and for each terrestrial cell of the Madingley model.

We ran the Madingley model at 2-degree resolution for a 100-year burn-in period, and then for a further 100 years for data collection. This length of time is sufficient for these models to be stable (Harfoot et al. 2014). We used default settings for the Madingley model, which did not factor in anthropogenic habitat loss or climate change (Harfoot et al. 2014). During the data collection period, the relevant demographic rates were recorded as running means. We performed 15 data-collection runs, and used an ensemble mean across the 100-year data collection period and across all 15 simulations in our downstream analyses. The results of these simulations are available as Supplementary Material DOI: 10.5061/dryad.h44j0zpvc.

Individual-Based Simulations and Generation Time

It is necessary to know generation length in years for each guild in the Madingley simulations. This is because the neutral-theory-based speciation rates are a probability per birth event whilst we wish to compare this to rates per species per million years. In order to obtain an accurate estimate of the emergent generation times within the Madingley model, we performed a set of independent, individual-based simulations on a spatially explicit grid using process rates collected from the Madingley simulations. To do this, for each guild, in each grid cell, $I = 1000$ independent adult individuals were simulated from month to month. The starting month was chosen randomly but in proportion to the fraction of juveniles that mature into adults in each month. For example, if half of juveniles mature into adults in May and the other half in June then half of the individual based simulations would likewise start in May and the other half in June. In a grid cell, any given "focal" adult either progressed to the following month, or died based on the mean mortality rate measured from the Madingley model simulations for that guild, location and month. Adult lifespan, in months, was recorded for any individuals that die. At each time step, the surviving focal adult may disperse to an adjacent grid cell depending on a random draw against the recorded mean dispersal rate out of that grid cell. The focal adult also stochastically produces offspring based on a Poisson process in each month. The number of offspring was given by the average number of births in the Madingley model, taking into consideration spatial and temporal heterogeneity in rates. Each offspring was then also simulated, in a similar manner to the adults, from the month and location of birth, until reaching reproductive maturity. Offspring were subject to juvenile mortality and dispersal checks

analogous to those of adults, but based on juvenile-specific rates collected separately from the Madingley model simulations. Juveniles are not reproductively active and instead they had a stochastic opportunity to mature based on the maturation rate for the grid cell they occupy in each specific month of the year. The number of time steps to maturity, in months, was recorded if the individual offspring did not die before maturing. We calculated generation length for each guild in month-long time steps that we then scaled to years. The generation length is the difference between the date of birth of an individual and the average date of birth of its offspring. Reproduction events happen throughout adult life so the average time of offspring birth is the midpoint of the part of an individual's life when it is a reproductive adult. Generation length can thus be calculated as the sum of 2 components: the mean time between birth and maturity of a juvenile, plus half of the time between maturation and death of an adult.

Metacommunity Richness with Protracted Speciation

After an initial genetic divergence between 2 potential species, it might take many generations and hundreds of thousands or millions of years before they can be considered fully distinct species (Weir and Price 2011). One way to include this mechanism in a neutral model is to consider an additional parameter τ, giving the duration of speciation as a number of generations. This mechanism is known as protracted speciation (Rosindell et al. 2010) and generalizes the point mutation mode of speciation from Neutral theory (Hubbell 2011). The speciation rate per individual organism, ν, (hereafter per capita speciation rate) may thus be smaller than the per capita speciation-initiation rate, μ, and the 2 are related by $\nu = \frac{\mu}{1+\tau}$ (Rosindell et al. 2010). We are following the conventions of Neutral Theory with μ as per capita speciation–initiation rate instead of extinction rate common in Macroevolutionary literature.

We obtain an analytical solution (see Supplementary Material) for the equilibrium metacommunity richness of a non-spatial neutral model with protracted speciation given by:

$$S = \theta \left\{ \left[\psi_0 \left(\frac{\theta \beta}{\theta + \beta} + J \right) - \psi_0 \left(\frac{\theta \beta}{\theta + \beta} \right) \right] - \left[\psi_0 (\beta + J) - \psi_0 (\beta) \right] \right\}, \quad (1)$$

where J is the community size, $\beta = \frac{J-1}{1+\tau}$, $\theta = \frac{(J-1)\mu}{(1-\mu)}$, and ψ_0 is the digamma function. Note how θ depends on the speciation-initiation μ, instead of the per capita speciation ν.

Whilst this solution is for a non-spatial model - we show by simulations (see Supplementary Material) that it also works as an approximation for the global species

richness in a spatially-explicit model with demographic rates parameterized from the Madingley model.

Endotherm Empirical Data

We obtained empirical data for species richness of terrestrial endotherms in each guild using the Elton-Traits 1.0 database of dietary and habitat requirements for birds and mammals (Wilman et al. 2014). We filtered the available data to ensure it was comparable to the ecology of simulated organisms in the Madingley model. Specifically, we removed all mammals that had "marine" foraging stratum category, and all of those whose diet consisted of more than 10% fish, as this resource is not explicitly modeled in the terrestrial-only simulations. To account for species that use freshwater wetlands and waterways, not explicitly modeled in Madingley, we also excluded species with any reference to "aquatic," "freshwater," or "glean" on the comments for foraging stratum. For birds, we excluded those assigned "Pelagic specialist," those that had "Vertebrates and Fish and Carrion" as dominant diet category and those whose diet consisted of more than 10% fish. We also removed birds whose prevalence of foraging on water surfaces (summing "below surface" and "just below surface") was greater than 50%. From a database with a total set of 9995 birds, we were left with 8677 (87%), and from 5403 mammals, 5084 (94%) remained.

We then categorized the remaining comprehensive list of terrestrial endotherms into 3 dietary categories: herbivore, carnivore, and omnivore. A species was considered a herbivore if the sum of the diet prevalence of fruit, nectar, seed, or other plant resources was equal to 100%, a carnivore if the sum was equal to 0%, and an omnivore for everything in between.

Speciation Rates Per Species Per Million Years

With the empirical values for endotherm richnesses and estimates of endotherm abundances from the Madingley model, we estimated speciation rates for each diet class at each interval of body mass. For each guild, we numerically solved equation 1 for the speciation-initiation rates μ, with S for empirical richness and J for Madingley abundance, and τ as a free parameter.

The speciation–initiation rates correspond to probabilities of initiating speciation for each birth/death event of an individual organism, thus not directly comparable to speciation rates estimated using phylogenetic methods, usually presented in units of per species (or per lineage) per million years. To obtain rates with comparable units, we first calculate speciation-completion rates $\nu = \frac{\mu}{1 + \tau}$, then perform the following transformation:

$$\nu^* = \frac{\nu}{2} \left(\frac{J}{S} \right) \left(\frac{1}{T_G} \right), \tag{2}$$

where ν is the speciation-completion rate (per individual per birth/death event), $\frac{J}{S}$ is the average number of individuals per species (considering simulated individual abundances and empirical species richnesses), and T_G is the generation time (in million years), obtained from the individual-based simulations using demographic rates probed from the Madingley simulations. The factor of 2 arises because we are modeling overlapping generations. As a result, the generation length is half the adult lifespan; relatedly, half of living adults are post reproduction and belong to an older generation (Rosindell et al. 2010). Equation 2 guarantees that ν^* expresses the speciation rate for a given guild in unit of per species per million years. Outputs are available as Supplementary Material.

Ectotherm Richness

The method that we applied to estimate speciation rates for endotherms, as functions of body mass and diet class, can be run in the other direction to infer ectotherm richnesses. First, we fitted power law functions separately for each diet class, to per species per million years speciation rates, and to generation times, as functions of body mass. We then extrapolated the results to obtain estimates of these quantities for smaller values of body mass, in particular those corresponding to the smaller body size guilds within ectotherm functional groups. This step involved assuming a power law relationship with speciation rate. Such a power law has been used previously (Etienne et al. 2012), we hope that as larger amounts of empirical data become available, future work will test the assumption further following (FitzJohn 2010; Etienne et al. 2012). For each guild of ectotherms, we have Madingley simulated abundances, the extrapolated values of speciation rate ν^*, and generation time T_G from our individual-based simulations. We thus obtain, for each guild, the speciation rates per individual per birth/death event, ν, as a function of the unknown species richness, S, by inverting equation 2. Thus, for each body mass guild, we obtain an expression for ν in terms of S that can be substituted into equation 1, allowing us to numerically solve the result for S. The resulting S provides an estimate of total species richness for that ectotherm guild. Outputs are available as Supplementary Material.

Ectotherm Empirical Data

Empirical data for reptile species richness was obtained from a database of extrapolated body masses, diets, and trophic levels (alongside other traits) of all vertebrate species (Etard et al. 2020). We counted the number of species at each interval of body size (with the same body size bins used to probe Madingley abundance distributions) for each trophic level (herbivore, carnivore, and omnivore). From this dataset we were also able to exclude species that were related to "Wetland,"

"Marine," or "Marine intertidal or costal supratidal" habitats, selecting only for terrestrial reptiles, which accounted for 9999 species. For amphibians, since we would not be able to exclude the use of aquatic habitats at a given stage during life time, these data were not included in our account of terrestrial ectotherms. At each body size interval, a number of species had undefined or unknown diet class. We distributed the count of unknown species into each diet class following the proportions of known diet classes for that body size interval. Some of the largest body size intervals had unknown diet class for all species, in which cases we assigned every species to carnivore, as they tend to be larger.

endothermic carnivores with body masses below 10^3 g were absent in our simulations (central panel, first row - Fig. 2). Abundances of carnivores peak at a body mass of 10^5 g, with a slight tendency of decreasing abundances at smaller and larger body masses.

Empirical species richness of endotherms, based on the EltonTraits database (Wilman et al. 2014) after our filtering process, peaked at a body mass of approximately 10^2 g for herbivores and omnivores, and at a body mass of around 10 g for carnivores (second row - Fig. 2). Numbers of species dropped sharply either side of the peak. The Madingley simulations supported carnivores and omnivores with large body masses (above $3 \cdot 10^5$ g) that are absent in the empirical species data.

Results

Madingley Abundances and Empirical Richnesses

The total abundance of herbivores and omnivores in the Madingley simulations shows a decreasing trend with increasing body mass, for body masses above 10^3 g (left and right panels, first row - Fig. 2). Herbivores further show a slight interior peak in abundance at just under 10^6 g despite an overall decreasing trend.

Terrestrial endothermic herbivores and omnivores with body masses below 10^2 g were scarce or absent in the Madingley simulated data. Similarly, terrestrial

Protracted Speciation Rates and Generation Times

For all diet classes, the relationship between speciation-initiation rates and body size was largely independent of the values of τ (Fig. 3). Although the values of the rates scale up and down with varying τ, the general pattern is kept constant, for each diet class, as a function of body size. Speciation-initiation rates, for all 3 diet classes, show a sharp decline with increasing body size for organisms of small size (below 10^3 g). After this, the herbivore speciation rate increases with body mass to form an interior peak between 10^3 g and 10^6 g, whilst
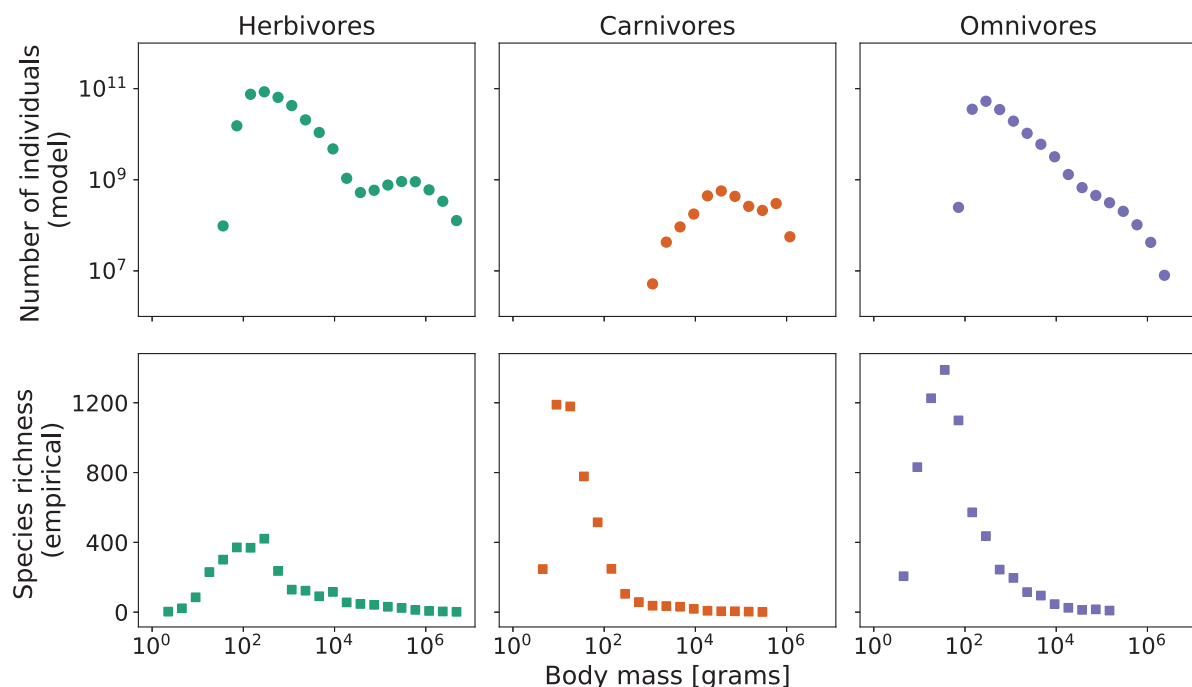

FIGURE 2. (First row) Average global abundances (in number of individuals) from the Madingley model at equilibrium for terrestrial endotherms. Standard errors are very small compared to the average values, therefore error bars are not visible. (Second row) Total empirical species richness for terrestrial endotherms. All plots are shown as a function of body mass: the midpoint of the body mass interval corresponding to each guild. Separate results are shown for 3 diet classes: herbivores (green, left), carnivores (orange, center), and omnivores (purple, right).
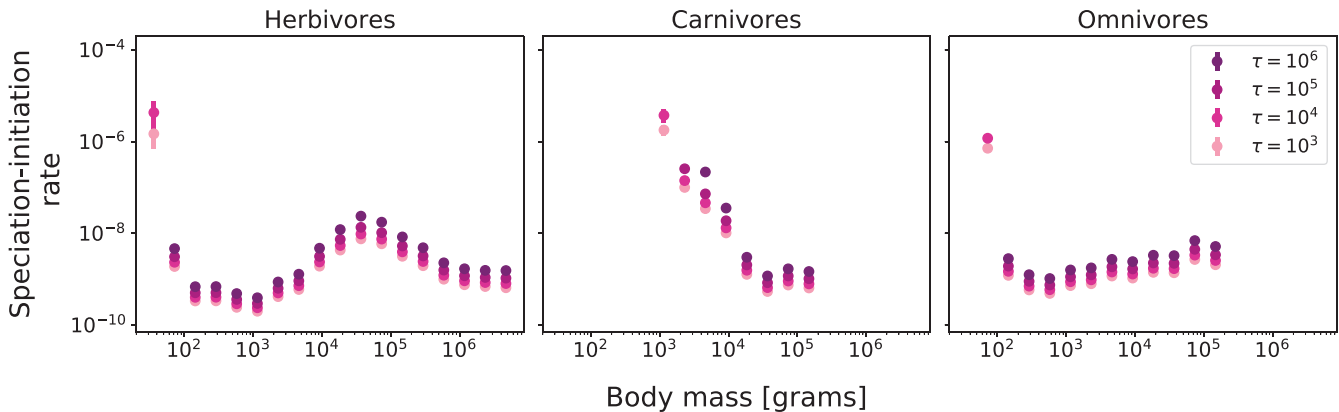
FIGURE 3. Numerical estimates of speciation-initiation rates (protracted speciation neutral model) for herbivore (left), carnivore (center), and omnivore (right) terrestrial endotherms, as a function of body mass. Results are shown for four different durations of protracted speciation: $\tau = 10^3$, 10^4, 10^5, and 10^6. Results are obtained as average values of speciation-initiation over 15 different samples of Madingley abundances and error bars correspond to one standard error of the mean. Often the error is smaller than the size of the point symbol and in these cases, it is not visible.

the omnivore speciation rate increases subtly with increasing body size, and the carnivore speciation rate remained flat (above 10^3 g for omnivores and above 10^4 g for carnivores).

Increasing values of τ led to increasing estimates of speciation-initiation rates, for all guilds in each of the dietary groups. For each diet class, some of the values of speciation-initiation rates for the smallest body mass guilds ($\tau = 10^5$ and $\tau = 10^6$) are not shown because equation 1 presented no numerical solution for μ (see Supplementary Material).

There are only negligible numbers of very small terrestrial endotherms predicted by the Madingley model simulations, particularly below 100 g (Fig. 2). As a result there is no modeled abundance data for those groups and no valid estimates of speciation rates. For carnivores, only guilds with body mass above 10^3 g show stable results for equilibrium abundances and thus there are no predicted speciation rates for carnivores below this body size (Fig. 3). Since the peaks for empirical richnesses for carnivores and omnivores are located between 10 and 100 g, speciation rates for a significant portion of the global biodiversity for these groups could not be evaluated by this method.

Estimated values of the generation times for all the guilds of terrestrial endotherms are below 20 months (Fig. 4). Across all guilds for which the 3 diet classes are present, omnivores show the highest generation times, followed by herbivores, and lastly carnivores. Carnivores and large-sized herbivores (above 10^4 g) are reasonably consistent with the theoretical allometric scaling for generation times, which predicts an increase of generation length with body mass as a power law with exponent 0.25 (Savage et al. 2004). For omnivores, the comparatively reduced slope indicates slower increase of generation time with body mass (see Supplementary Material for a comparison with empirically estimated generation times).
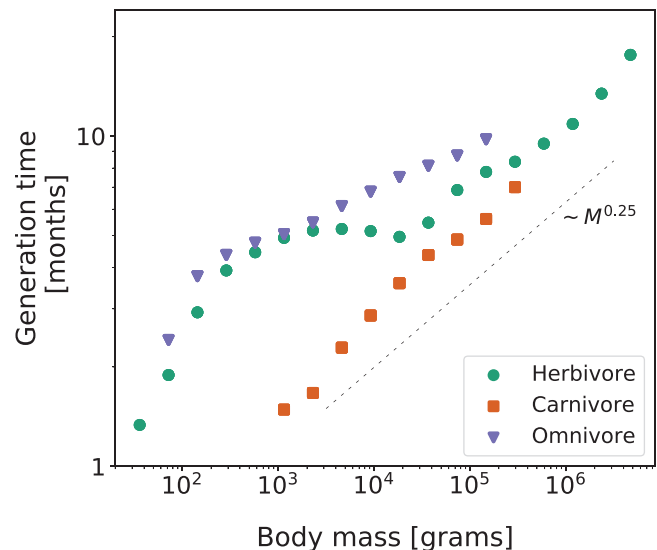

FIGURE 4. Generation times for terrestrial endotherm guilds. The times were estimated from individual-based simulations using stationary demographic rates in the Madingley model, as a function of body size. Results are shown for herbivores (green circles), carnivores (orange squares), and omnivores (purple triangles). The dashed line shows a reference slope for the allometric scaling $\sim M^{0.25}$ with arbitrary intercept.

Speciation Rates for Terrestrial Endotherms

Speciation rates, converted to units of per species per million years, show a consistent pattern of decline with body mass in the 3 diet classes of terrestrial endotherms (Fig. 5). In the case of the herbivore diet class, there is additionally an almost flat relationship between body size and speciation rate at intermediate body sizes. For most guilds, speciation-initiation varies in a range smaller than one order of magnitude for all the assessed values of τ (Fig. 3). As a result, an inversely proportional relation approximately holds between τ and speciation rate per species per million years.
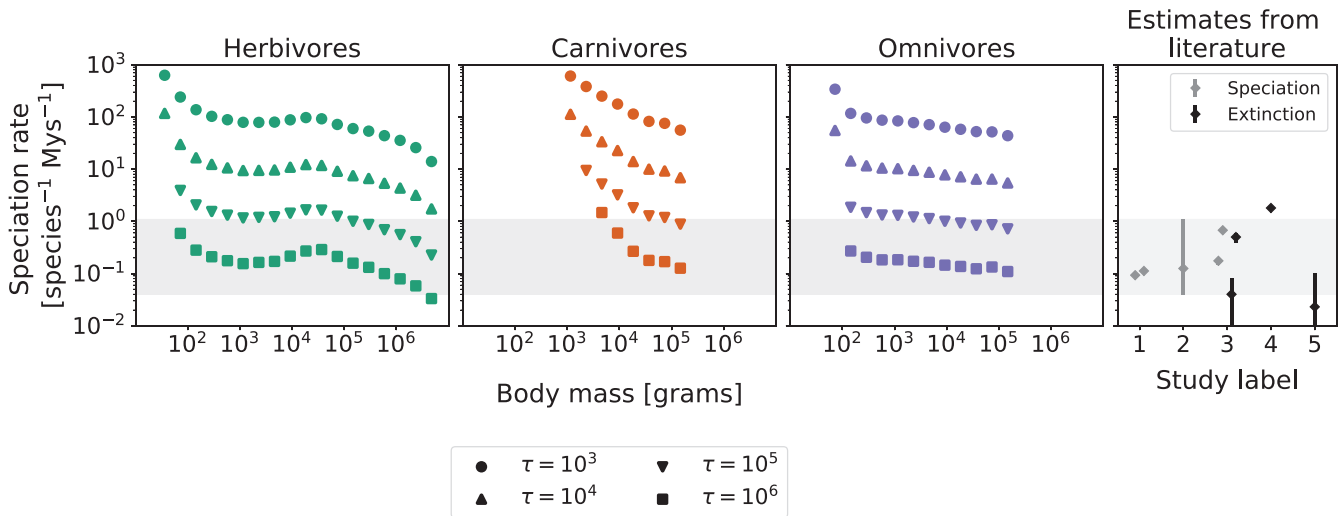
FIGURE 5. (First 3 panels) Speciation rates per species per million years as a function of body mass for 3 diet classes of terrestrial endotherms. For each class, the rates are calculated for four distinct values of speciation-completion time: $\tau = 10^3$, 10^4, 10^5, and 10^6. Rates for each guild correspond to mean values over 15 estimates, using stationary abundances from different Madingley simulations. Values for the standard errors of the mean are very small compared to the mean values, therefore error bars are not visible. (Rightmost panel) Estimates of speciation and extinction rates (gray and black diamonds, respectively, in units of event per species per million years) obtained from previous studies, labeled as follows: (1) Rolland et al. (2014), (2) Rabosky et al. (2015), (3) Weir and Schluter (2007), (4) Barnosky et al. (2011), and (5) De Vos et al. (2015).

The comparison between the 3 diet classes also shows that, while herbivores and omnivores present similar values of speciation rates for the same body size group, speciation rates for carnivores are often higher, for the interval where the rates could be estimated for the 3 groups (approximately between 10^3 g and 10^5 g). The difference is particularly clear for smaller-bodied carnivores (see Supplementary Material).

Direct comparison is also possible with estimates of speciation rates for birds and mammals from previous works (Fig. 5 - gray diamonds, rightmost panel). Here we focus on rates inferred from reconstructed molecular phylogenies (but see also (Alroy 1999) for rates directly inferred from fossil data). The speciation rates we obtain with our method are consistent with the range of values obtained from the literature through entirely different methods, particularly for values of τ equal to 10^5 and 10^6 (although not shown in Fig. 5, rates estimated from fossil data in (Alroy 1999) also correspond the same range).

By using equation 1 to estimate speciation rates, we implicitly assume that the empirical patterns for richness correspond to equilibrium richness of the neutral model with protracted speciation. In a neutral model, net zero diversification rate is reached at equilibrium, when speciation rates equal extinction rates. Thus, the values we obtain for speciation rates as functions of body mass in Figure 5 also correspond to extinction rates (under the assumptions of our model). Direct comparison with estimates of baseline extinction rates from the literature (Fig. 5 - black diamonds, rightmost panel) also reveals that extinction rates obtained via our method are consistent with those

obtained from phylogenetic analysis, for values of $\tau = 10^5$ and 10^6.

Mechanistic Estimates of Ectotherm Richness

Fitted plots and parameter tables for the power law functions of speciation rate per species per million years can be seen in the Supplementary Material. We have estimated richnesses for ectotherms, as functions of body mass and diet, by extrapolating these functions for $\tau = 10^5$ and 10^6, the 2 values of speciation-completion time which are more consistent with previous estimates from phylogenetic approaches (see Fig. 5). The results for ectotherm richnesses can be seen in Figure 6, which also shows comparative data on empirical richnesses of iteroparous ectotherms of large body size (see Methods). As a general trend, species richness decreases with increasing body mass for all groups, at least for larger values of body mass. At the small body size end of the spectrum there is a relatively brief band where this relationship is reversed. For semelparous ectotherms, while herbivores and omnivores present similar values of abundance at each body mass bin, values of speciation rates for herbivores are greater than the ones for omnivores (for the same values of τ) in the body mass range from 10^{-2} to 10^4 g. For semelparous carnivores, although values of abundance are orders of magnitude lower in comparison to herbivores and omnivores, speciation rates are higher, for values of body mass below 10^5 g. Summing the richnesses of all body mass intervals for the 3 diet classes, we have total global richnesses for semelparous ectotherms ranging from $9.97 \cdot 10^5$ to
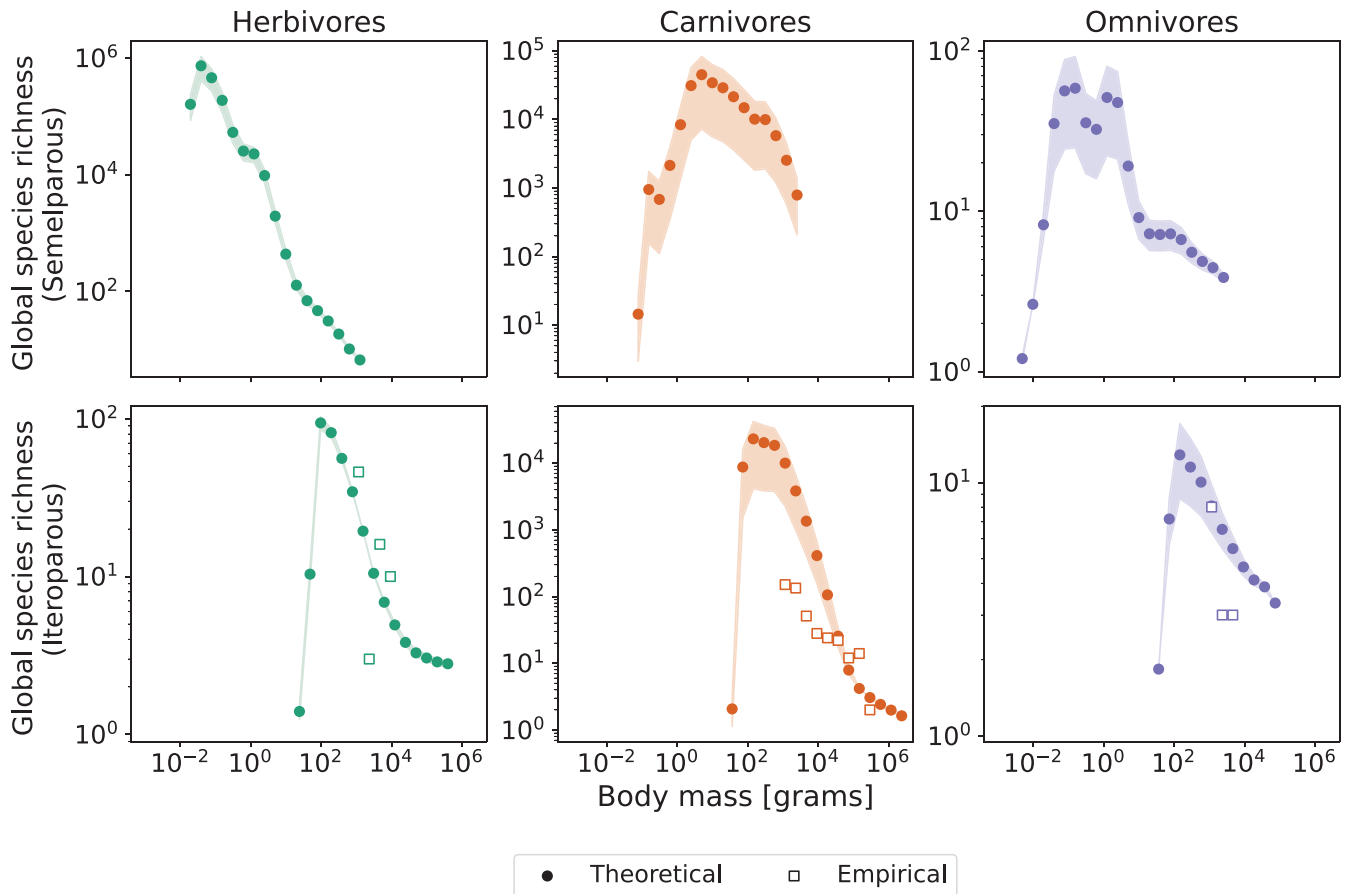
FIGURE 6. Global species richnesses for terrestrial ectotherms, as functions of body mass and diet. Results are shown for 2 reproduction strategies, semelparous (first row) and iteroparous (second row), following the definitions of functional groups in the Madingley model. Shaded regions correspond to the range of estimated richnesses for each body mass for the 2 values of speciation-completion times used ($\tau = 10^5$ and 10^6), while circles correspond to the mean values for these ranges. Empty squares on the second row show empirically estimated richnesses for reptiles above 1 kg obtained in Etard et al. (2020) (see Methods).

$2.75 \cdot 10^6$ species, and for iteroparous ectotherms ranging from $1.75 \cdot 10^4$ to $1.56 \cdot 10^5$ species (the smallest values corresponding to $\tau = 10^6$ and the highest, to $\tau = 10^5$). The total number of terrestrial animals, including our predicted numbers of ectotherms, and our empirically derived number of $13,703$ endotherms (given particular diet restrictions and excluding marine or freshwater environments - see Methods), was between $1.03 - 2.92$ million species, depending on the value of τ.

DISCUSSION

In this study, we sought to connect two previously unconnected areas of theory to address two questions that have so far been approached independently. The "Madingley model" (Harfoot et al. 2014) is a first-of-its-kind general ecosystem model, able to make mechanistic global-scale predictions about broad functional groups of organisms on land and in the ocean. One key limitation to the Madingley Model, however, is that it

omits species identities and so cannot make predictions about species richness or speciation. In contrast, ecological neutral models (Hubbell 2011) do not incorporate the functional differences that are captured by the Madingley model, but focus instead on making predictions about species, including speciation and extinction rates. By combining the two, we introduce a body of mechanistic theory that operates tractably at the global level and also includes the species concept. In this study, we applied our approach to estimate speciation rates of terrestrial endotherms as a function of diet class and body size, and to estimate the total diversity of terrestrial ectotherms, including all undescribed species.

Per Capita Speciation and Generation Length

Our results for Per capita per-birth speciation-initiation rates μ represent an interim result from our analysis pipeline, relevant only in the context of neutral theory. It is still worthwhile to consider the mechanistic reasons behind the patterns in μ that we observe. These

seem to be mostly arising from fluctuations in the numbers of individual organisms for different guilds predicted by the Madingley model. The hump in μ for intermediate body sizes of herbivores appears to correspond to the slight dip in the total number of individual organisms at the same body size, as estimated by the Madingley model. Similarly, our result that small carnivores diversify faster than herbivores or omnivores of the same body size coincides with there being fewer individual organisms without there being proportionately fewer species. Whilst the values of μ are not typically studied, it seems plausible to us that the empirical relationship with body size could be hump-shaped where there is a dip in numbers of individuals without a corresponding dip in numbers of species. This case is what our model shows.

To translate these per-birth speciation rates into a rate per species per million years required us to know both number of individuals per species and number of generations per million years. To derive the latter, we used generation lengths in years predicted by the combined use of the Madingley model and our individual-based simulations. Our estimated values of the generation times for all the guilds of terrestrial endotherms are below 20 months (Fig. 4). This is rather short, especially for guilds of large body sizes, and is consistent with the accelerated pace of life predicted for organisms in the Madingley model, as compared to empirical estimates (Harfoot et al. 2014). The relationship between generation length and body size did, however, show comparable results to a power law with exponent 0.25, consistent with previous expectations (Savage et al. 2004). For our main results in terms of species numbers, altering generation length by a factor probably has little effect. To see why this is the case, consider a halving of estimates for generation length across all species. This would double speciation rates per million years for endotherms due to there being twice as many generations per million years. The extrapolated speciation rates per million years for ectotherms would also be doubled as they are based on the values for endotherms. When these rates get translated back to a per generation basis, however, we are dividing the doubled speciation rate per million years by the number of generations in a million years, which has also doubled. This would cancel out the doubling and return speciation rate per generation back to something close to where it would have been with the original generation length.

Speciation Rate Variability with Body Size and Diet Class

Our estimations of speciation rate per species per million years, as a function of body mass and diet class depend on the speciation-completion time, τ (the time it takes to form 2 separate species from 2 lineages that started to diverge). As a result, we have a range of speciation rates for the same diet class and body mass interval as τ varies (Fig. 5). However, while the resulting curves in Figure 5 move up and down with τ, they do not

change shape. Thus, the qualitative way that speciation rates vary with body size and diet class is independent of the value of τ, and thus remains a robust finding of our models.

In general, previous work across different taxa has reported mixed relationships that focus on diversification rate, species richness, and body size (Orme et al. 2002; Wollenberg et al. 2011; Feldman et al. 2016). Previous studies suggest that diversification may decrease with increasing body size, but may also be humped or with no relationship. Previous work has also approached the question of how diversification may vary with diet class, suggesting that herbivores diversify fastest, followed by carnivores and then omnivores (Price et al. 2012). What is noteworthy about previous work is the focus on net diversification, rather than on speciation, which is notoriously difficult to pick apart from extinction (Louca and Pennell 2020). There is a general agreement that the answers remain unresolved. As a result, these previous works are neither supportive nor in contradiction with our results about speciation rate and its relationship with body size and diet. We did not find a single simple relationship between body size, diet, and speciation rate, but certain results did stand out. For example, speciation rates per species per million years were generally higher with smaller body sizes (Fig. 5). There are several factors contributing to this based on the mechanisms of our underlying models. Firstly, the Per capita per-generation speciation rates are highest for the smallest bodied species, though don't always increase with decreasing body size so this factor alone is insufficient (Fig. 3). Secondly, the shorter generation time of smaller bodied species (Etienne et al. 2012) leave more generations and thus more opportunities for speciation per million years. Thirdly, the larger population size of small-bodied species would have a positive effect because there are more individuals who could potentially start the speciation process. We also found that smaller carnivores have higher speciation rates than herbivores and omnivores of the same body size. This may be because the higher values of μ for carnivores are not entirely cancelled out when we translate μ back into speciation rates per species per million years.

Quantitative Speciation Rates and Background Extinction Rates

Overall, our speciation rates per species per million years, regardless of diet class and body size, are consistent with independent estimates for endotherms obtained from studies using different phylogenetic methods that do attempt to separate speciation from net diversification. For example, Rolland et al. (2014) obtain 95% credibility intervals for posterior distributions on speciation rates that range, approximately, from 0.085 to 0.101 for temperate mammals and from 0.107 to 0.116 for tropical mammals (study 1 – Fig. 5). Rabosky et al. (2015), working with bayesian inference on New World Birds phylogenetic data obtain per-taxon rates

that range from 0.04 to 0.11 new species per million years (study 2 – Fig. 5). Weir and Schluter (2007) estimate intervals of speciation rates for birds and mammals varying with latitude, with estimated per-lineage per-million years rates of 0.15-0.2 at the Equator and 0.6-0.75 at 50° latitude, N or S (study 3 – Fig. 5). Overall, speciation rates for endotherms obtained from previous studies are within a range from 0.04 to 0.11, which corresponds to the range seen for τ between 10^5 and 10^6 (gray rectangles in Fig. 5). These values of τ are broadly consistent with expectations for the speed of segregation of lineages (Weir and Price 2011) though smaller values of τ might be plausible and would be consistent with larger underlying background rates of speciation and extinction. This speed should certainly be less than the expected waiting time between successful speciation events, but should also not be small, which would correspond to a generally unrealistic scenario (Rosindell et al. 2010). Our model, in line with applications of protracted speciation to neutral theory (Rosindell et al. 2010), has a fixed duration of speciation. In contrast, applications of protracted speciation to models of phylogenetic trees (Etienne and Rosindell 2012; Etienne et al. 2014), and incorporating the mechanistic effects of gene flow (Rosindell and Phillimore 2011; Tao et al. 2021), have tended to have stochastic completion of speciation events, resulting in a distribution of possible waiting times to speciation. Further work could consider the implications of alternative implementations of the protracted speciation concept, however, whilst τ itself is so broadly variable, and so weakly influencing our results, it would not be a priority to make the variable stochastic.

Under our neutral models, a dynamic equilibrium between speciation and extinction is assumed for any particular guild. This enables us to equate our speciation rates directly to extinction rates per species per million years and to a net diversification rate of zero. Retaining the same range of τ between 10^5 and 10^6 the values we obtain for background extinction rates also present a reasonable correspondence with the range of extinction rates obtained from previous studies, ranging from 0.0 to 1.8 extinctions per species per million years (or equivalently per million species per year, the more usual unit for background extinction rate) (Weir and Schluter 2007; Barnosky et al. 2011; De Vos et al. 2015) (studies 3–5 – Fig. 5). In the context of this study, forcing net zero diversification rates provides a new perspective on speciation and extinction as well as how they vary with body size. The approach avoids the time scale dependence of speciation rates that have been pointed out when estimating rates from phylogeny (Harmon et al. 2021; Louca et al. 2022). This is because our speciation rate is determined based on what is required to explain the given species richness at equilibrium, given the number of individual organisms in the guild. Future work may consider relaxing the dynamic equilibrium assumption which would enable speciation rates to change through time. Finding true underlying speciation rates, and background extinction rates, remains a challenge. We suggest that both inferential methods and mechanistic models of different kinds are needed, and should ideally get consistent results, in order to provide convincing answers through a 'mixed approach'.

Total Species Richness of Terrestrial Animals

The possibility of reversing the neutral model component of our pipeline to estimate species richness for ectotherms provides a novel approach to investigate biodiversity patterns of undersampled groups. Our results for estimated total species richness are sensitive to changes in speciation rates (per species per Mys) and, to a lesser extent, to values of ectotherm abundances (see Supplementary Material). This explains the large difference in predicted numbers of species between omnivores and the other 2 diet classes. Analogous reasoning can be used to interpret the differences between diet groups for iteroparous ectotherms. The positive correlation between richness and body mass for smaller values of body mass is not necessarily realistic, but is associated with the low abundances for small-bodied organisms in Madingley's stationary distributions, a known limitation of the Madingley model (Harfoot et al. 2014), rather than of the way it is used in this application.

Overall, our estimated number of terrestrial species is between 1.03 and 2.92 million, dominated by guilds of ectotherms that likely correspond to arthropods. These results are broadly consistent with current estimates of extant terrestrial arthropods of 7 million species (Stork 2018). Our estimated numbers of iteroparous ectotherms, ranging from approximately 17,500 to 156,000 also compare well to extant reptile and amphibian fauna of 11,570 and 8,482 species, respectively (Uetz et al. 1995; AmphibiaWeb 2022). This comparison, however, should be taken with caution because many iteroparous ectotherms will also be arthropods, and conversely many amphibians will not be terrestrial.

The empirical estimates of species richness for reptiles with body size above 1000 g should exclude the majority of arthropods in the iteroparous ectotherms group (Fig. 6). Most amphibians will also be excluded given the constraints to body sizes above 1000 g and terrestrial environments. These numbers will thus be suitable as an initial validation of our theoretical predictions of species richness for groups in the same body size intervals. Apart from iteroparous carnivores below 10^4 g, theoretical predictions and empirical estimates of species richness for iteroparous ectotherms do not differ by more than one order of magnitude. Further validation of these results will be possible in the future when new data on ectotherm richnesses are gathered or when the granularity at which general ecosystem models represent different taxonomic divisions enables predictions for more finely divided functional groups.

Limitations and Potential Future Work

Since the publication of the original Madingley model, it has been used in many applications, such as understanding the effect of perturbations to ecosystems, from habitat loss and fragmentation (Newbold et al. 2020; Bartlett et al. 2016), large carnivore loss (Hoeks et al. 2020) and bushmeat hunting (Barychka et al. 2021). It was also applied to investigate the impact of arbuscular mycorrhizal fungi on higher trophic levels (Stevens et al. 2018). As more data becomes available, the possibility of reassessing some of Madingley's limiting assumptions might open a broad range of potential lines of investigation.

The version of the Madingley model from which we derived our data assumes a pristine world in which there has been no anthropogenic change. Given our aims to understand historic speciation rates and background extinction rate (without anthropogenic species loss), this assumption seems justified. We calibrated our speciation rates to match presently extant terrestrial endotherms rather than the numbers of terrestrial endoterms that existed prior to anthropogenic influences. This will mean that our total numbers of species take into account anthropogenic change to some extent. The difference caused by this is probably relatively small for most body sizes since only a very small percentage of described species have so far been declared extinct and our pipeline only requires species numbers (not empirical abundances of individuals for each species). Increasing numbers of endangered yet extant species would not affect our results. An exception would be large-bodied species where hunting has caused a large proportion of extinctions due to anthropogenic change. This is one of the reasons why the Madingley model supported the existence of some large-bodied endotherm groups not matched by our empirical data (Fig. 2). It would be possible to account for recently extinct species but this would require a comprehensive database of all recently extinct endothermic life, together with body size and diet data. Future work could more explicitly incorporate anthropogenic change and study its effects. For example, by changing the environmental and landscape input data in Madingley, according to projected scenarios of climate change. Similarly, habitat loss could be simulated via removal of a proportion of primary productivity from the landscape for use in food production and support of domesticated animals (Newbold et al. 2020).

Another limitation in our approach is the lack of small-bodied organisms in the stationary abundances in the Madingley model. This affects not only the estimation of speciation rates for endotherm body masses lower than 100 g, but also results in larger errors in the estimation of ectotherm richness by extrapolation of the endotherm rates. Stationary distributions of ectotherms in Madingley are also underrepresented in a large interval in comparison to the lower bounds allowed in Madingley for these groups (lower bounds for body masses of semelparous and iteroparous ectotherms in Madingley are 0.0004 g and 1 g, respectively). There are numerous possible drivers of the lack of abundance of small organisms in Madingley. For example, the lack of temperature-dependence for foraging parameters (Rall et al. 2012) may wrongly disadvantage small-bodied organisms. The high relative metabolic costs may impose a disproportionately large additional energetic burden on small organisms (Sibly et al. 2012). Vegetation in Madingley is not vertically structured, so there is no distinct rainforest canopy for example. Often it is vertical structuring that creates new niches favoring small-bodied taxa (Krause et al. 2022). In the natural world, smaller organisms are frequently able to exploit flushes of high energy resources such as nectar, fruits, and seeds, all of which are not explicit in the Madingley model. Another possibility is that since modeled endotherms in Madingley are active for one hundred percent of a model time step and cannot seek metabolic refuge to limit their energy expenditure, they cannot optimize their energy budgets as natural organisms such as hummingbirds (Payne 2010) and bats (Eisenberg 1981) do by way of torpor and crepuscular behaviors. The effect of all these drivers on Madingley biodiversity distributions should be explored in future work.

A promising line of investigation resides on the improvement of the performance of spatial neutral models. Here we used the analytical solution of non-spatial neutral models as an approximation to the global richness, with which we estimated speciation rates for endotherms and richnesses for ectotherms. Although it can be shown that the non-spatial analytical richness seems a reasonable first approximation for the global richness in a spatial model (see Supplementary Material), we know that abundance distributions in Madingley are strongly affected by spatial heterogeneities in availability of resources and species dispersal kernels. The main reason to use this approximation is the heavy computational cost of performing spatial neutral simulations (Thompson et al. 2020), with values of speciation rates and abundance needed to match the empirical patterns. In these spatial models, the introduction of optimizations such as Gillespie algorithms may lead to a significant gains in performance, allowing estimates of spatial richness distributions instead of only total global richness. Developments on this front could benefit not only our method's estimates for speciation rates and undescribed species richnesses, but the field of ecosystem modeling as a whole, with mechanistic models playing a central role in producing theoretical and applied advancements.

Conclusion

In this work, we have synthesized two mechanistic models to connect previously disparate fields of ecological theory. The result is a new pipeline with synergistic models capable of making predictions about large-scale

and partially observed phenomena, illustrated here with a study of species richness and speciation rates. Our method opens the possibility of exploring drivers of speciation and background extinction from a mechanistic approach; this opens up the possibility of making emergent predictions around other evolutionary processes and questions. The deeper potential of our approach is that it paves the way to incorporate anthropogenic change, and thus mechanistically predict anthropogenic extinctions with potential conservation applications. This line of investigation is hard to perform with traditional models based on phylogenetic inference, since they are not underpinned by a general ecosystem model or process-based ecologica theory.

Perhaps what is most remarkable about our results is that both species richness and speciation rate estimates for all terrestrial animals have been obtained using only limited data from larger endotherms and their speciation rates, with the rest of the predictive process being grounded in mechanistic models. Our hope is that this work will pave the way for future general ecosystem model and neutral model combinations. Not just to apply this to the marine and freshwater realms, but also as part of an ongoing interest in general ecosystem models, that can now include mechanistic predictions about species diversity. Whilst this does involve making many assumptions, it is likely the only approach that will lead to tractable process-based models of global species diversity from first principles. The addition of neutral theory to general ecosystem models introduces the species concept and brings the original vision of general ecosystem models one step closer to reality.

Supplementary Material

Supplementary material, including data files and/or online-only appendices, can be found in the Dryad data repository: http://datadryad.org, and http://dx.doi.org/10561/dryad.h44j0zpvc.

Conflict of Interest

The authors declare no conflicts of interest.

References

Alroy J. 1999. The fossil record of North American mammals: evidence for a paleocene evolutionary radiation. Syst. Biol. 48:107–118.

AmphibiaWeb. 2022. Amphibiaweb. https://amphibiaweb.org/ Accessed: November 07, 2022.

Barnosky A. D., Matzke N., Tomiya S., Wogan G. O., Swartz B., Quental T. B., Marshall C., McGuire J. L., Lindsey E. L., Maguire K. C., Mersey B., and Ferrer E. A. 2011. Has the earth's sixth mass extinction already arrived? Nature 471:51–57.

Bartlett L. J., Newbold T., Purves D. W., Tittensor D. P., and Harfoot M. B.. 2016. Synergistic impacts of habitat loss and fragmentation on model ecosystems. Proc. R. Soc. B: Biol. Sci. 283:20161027.

Barychka T., Mace G. M., and Purves D. W. 2021. The Madingley general ecosystem model predicts bushmeat yields, species extinction rates and ecosystem-level impacts of bushmeat harvesting. Oikos 130:1930–1942.

Billaud O., Moen D., Parsons T. L., and Morlon H. 2020. Estimating diversity through time using molecular phylogenies: Old and species-poor frog families are the remnants of a diverse past. Syst. Biol. 69:363–383.

Bouchet P. and Duarte C. M. 2006. The exploration of marine biodiversity: scientific and technological challenges. Fundación BBVA 33:1–34.

Caswell H. 1976. Community structure: a neutral model analysis. Ecol. Monogr. 46:327–354.

Chisholm R., Fung T., Chimalakonda D., and O'Dwyer J. 2016. Maintenance of biodiversity on islands. Proc. R. Soc. B: Biol. Sci. 283:20160102.

Chisholm R. and Pacala S. 2010. Niche and neutral models predict asymptotically equivalent species abundance distributions in high-diversity ecological communities. Proc. Natl. Acad. Sci. 107:15821–15825.

Connolly S. R., Keith S. A., Colwell R. K., and Rahbek C. 2017. Process, mechanism, and modeling in macroecology. Trends Ecol.& Evol. 32:835–844.

De Vos J. M., Joppa L. N., Gittleman J. L., Stephens P. R., and Pimm S. L. 2015. Estimating the normal background rate of species extinction. Conserv. Biol. 29:452–462.

Eisenberg J. F. 1981. The mammalian radiations: an analysis of trends in evolution, adaptation, and behavior. The University of Chicago Press, Chicago and London.

Etard A., Morrill S., and Newbold T.. 2020. Global gaps in trait data for terrestrial vertebrates. Global Ecol. Biogeogr. 29:2143–2158.

Etienne R., de Visser S., Janzen T., Olsen J., Olff H., and Rosindell J. 2012. Can clade age alone explain the relationship between body size and diversity? Interface Focus 2:170–179.

Etienne R. S., Morlon H., and Lambert A. 2014. Estimating the duration of speciation from phylogenies. Evolution 68:2430–2440.

Etienne R. S. and Rosindell J. 2012. Prolonging the past counteracts the pull of the present: protracted speciation can explain observed slowdowns in diversification. Syst. Biol. 61:204.

Feldman A., Sabath N., Pyron R., Mayrose I., and Meiri S. 2016. Body sizes and diversification rates of lizards, snakes, amphisbaenians and the tuatara. Global Ecol. Biogeogr. 25:187–197.

FitzJohn R. 2010. Quantitative traits and diversification. Syst. Biol. 59:619–633.

Gaston K. J. 1991. The magnitude of global insect species richness. Conserv. Biol. 5:283–296.

Gaston K. J. and Blackburn T. M. 2000. Pattern and process in macroecology. vol. 414. Wiley Online Library.

Grimm V. 1999. Ten years of individual-based modeling in ecology: what have we learned and what could we learn in the future? Ecol. Model. 115:129–148.

Harfoot M. B., Newbold T., Tittensor D. P., Emmott S., Hutton J., Lyutsarev V., Smith M. J., Scharlemann J. P., and Purves D. W. 2014. Emergent global patterns of ecosystem structure and function from a mechanistic general ecosystem model. PLoS Biol. 12:e1001841.

Harmon L. J., Pennell M. W., Henao-Diaz L. F., Rolland J., Sipley B. N., and Uyeda J. C.. 2021. Causes and consequences of apparent timescaling across all estimated evolutionary rates. Ann. Rev. Ecol. Evol. Syst. 52:587–609.

Hawksworth D. L. 1991. The fungal dimension of biodiversity: magnitude, significance, and conservation. Mycol. Res. 95:641–655.

Herrera-Alsina L., Van Els P., and Etienne R. 2019. Detecting the dependence of diversification on multiple traits from phylogenetic trees and trait data. Syst. Biol. 68:317–328.

Hoeks S., Huijbregts M. A., Busana M., Harfoot M. B., Svenning J.-C., and Santini L. 2020. Mechanistic insights into the role of large carnivores for ecosystem structure and functioning. Ecography 43:1752–1763.

Holling, C. S. 1959. Some characteristics of simple types of predation and parasitism. Canadian Entomol. 91:385–398.

Hubbell, S. P. 2011. The unified neutral theory of biodiversity and biogeography (mpb-32). *in* The Unified Neutral Theory of Biodiversity and Biogeography (MPB-32). Princeton University Press.

Jetz W., Thomas G., Joy J., Hartmann K., and Mooers A. 2012. The global diversity of birds in space and time. Nature 491: 444–448.

Krause J., Harfoot M., Hoeks S., Anthoni P., Brown C., Rounsevell M., and Arneth A. 2022. How more sophisticated leaf biomass simulations can increase the realism of modelled animal populations. Ecol. Model. 471:110061.

Louca S., Henao-Diaz L. F., and Pennell M. 2022. The scaling of diversification rates with age is likely explained by sampling bias. Evolution 76:1625–1637.

Louca S. and Pennell M. W. 2020. Extant timetrees are consistent with a myriad of diversification histories. Nature 580:502–505.

May R. M. 1988. How many species are there on earth? Science 241:1441–1449.

Mora C., Tittensor D. P., Adl S., Simpson A. G., and Worm B. 2011. How many species are there on earth and in the ocean? PLoS Biol. 9:e1001127.

Morlon H. 2014. Phylogenetic approaches for studying diversification. Ecol. Lett. 17:508–525.

Newbold T., Tittensor D. P., Harfoot M. B., Scharlemann J. P., and Purves D. W. 2020. Non-linear changes in modelled terrestrial ecosystems subjected to perturbations. Sci. Rep. 10:14051.

Orme C., Isaac N., and Purvis A. 2002. Are most species small? Not within species-level phylogenies. Proc. R. Soc. B: Biol. Sci. 269:1279–1287.

Payne R. 2010. Handbook of the birds of the world. Wilson J. Ornithol. 122:627–629.

Penn J. and Deutsch C. 2022. Avoiding ocean mass extinction from climate warming. Science 376:524–526.

Pennell M. W. and Harmon L. J. 2013. An integrative view of phylogenetic comparative methods: connections to population genetics, community ecology, and paleobiology. Ann. N. Y. Acad. Sci. 1289:90–105.

Price S., Hopkins S., Smith K., and Roth V. 2012. Tempo of trophic evolution and its impact on mammalian diversification. Proc. Natl. Acad. Sci. 109:7008–7012.

Purves D., Scharlemann J., Harfoot M., Newbold T., Tittensor D., Hutton J., and Emmott S. 2013. Time to model all life on earth. Nature 493:295–297.

Pyron R. A. and Burbrink F. T. 2013. Phylogenetic estimates of speciation and extinction rates for testing ecological and evolutionary hypotheses. Trends Ecol. & Evol. 28:729–736.

Rabosky D., Grundler M., Anderson C., Title P., Shi J., Brown J., Huang H., and Larson J. 2014. Bamm tools: an r package for the analysis of evolutionary dynamics on phylogenetic trees. Methods Ecol. Evol. 5:701–707.

Rabosky D. L. 2010. Extinction rates should not be estimated from molecular phylogenies. Evol: Int. J. Org. Evol. 64:1816–1824.

Rabosky D. L., Title P. O., and Huang H. 2015. Minimal effects of latitude on present-day speciation rates in new world birds. Proc. R. Soc. B: Biol. Sci. 282:20142889.

Rall B. C., Brose U., Hartvig M., Kalinkat G., Schwarzmüller F., Vucic-Pestic O., and Petchey O. L. 2012. Universal temperature and body-mass scaling of feeding rates. Phil. Trans. R. Soc. B: Biol. Sci. 367:2923–2934.

Raven P. 1985. Disappearing species-a global tragedy. Futurist 19:8–14.

Rolland J., Condamine F. L., Jiguet F., and Morlon H. 2014. Faster speciation and reduced extinction in the tropics contribute to the mammalian latitudinal diversity gradient. PLoS Biol. 12:e1001775.

Rosindell J., Cornell S. J., Hubbell S. P., and Etienne R. S. 2010. Protracted speciation revitalizes the neutral theory of biodiversity. Ecol. Lett. 13:716–727.

Rosindell J. and Phillimore A. B. 2011. A unified model of island biogeography sheds light on the zone of radiation. Ecol. Lett. 14:552–560.

Savage V., Gillooly J., Brown J., West G., and Charnov E. 2004. Effects of body size and temperature on population growth. Am. Nat. 163:429–441.

Sibly R. M., Brown J. H., and Kodric-Brown A. 2012. Metabolic ecology: a scaling approach. John Wiley & Sons.

Stevens B. M., Propster J., Wilson G. W., Abraham A., Ridenour C., Doughty C., and Johnson N. C. 2018. Mycorrhizal symbioses influence the trophic structure of the Serengeti. J. Ecol. 106:536–546.

Stork N. E. 1993. How many species are there? Biodivers. & Conserv. 2:215–232.

Stork N. E. 2018. How many species of insects and other terrestrial arthropods are there on Earth. Ann. Rev. Entomol. 63:31–45.

Tao R., Sack L., and Rosindell J. 2021. Biogeographic drivers of evolutionary radiations. Front. Ecol. Evol. 9:644328.

Thompson S. E., Chisholm R. A., and Rosindell J. 2020. Pycoalescence and rcoalescence: packages for simulating spatially explicit neutral models of biodiversity. Methods Ecol. Evol. 11:1237–1246.

Uetz P., Hallermann J., and Hosek J. 1995. The reptile database. https://reptile-database.reptarium.cz/ Accessed: November 07, 2022.

Weir J. T. and Price T. D. 2011. Limits to speciation inferred from times to secondary sympatry and ages of hybridizing species along a latitudinal gradient. Am. Nat. 177:462–469.

Weir J. T. and Schluter D. 2007. The latitudinal gradient in recent speciation and extinction rates of birds and mammals. Science 315:1574–1576.

Williams R., Anandanadesan A., and Purves D. 2010. The probabilistic niche model reveals the niche structure and role of body size in a complex food web. PloS one 5:e12092.

Wilman H., Belmaker J., Simpson J., de la Rosa C., Rivadeneira M. M., and Jetz W. 2014. Eltontraits 1.0: species-level foraging attributes of the world's birds and mammals: Ecol. Archiv. e095-178. Ecology 95:2027–2027.

Wollenberg K., Vieites D., Glaw F., and Vences M. 2011. Speciation in little: the role of range and body size in the diversification of Malagasy Mantellid frogs. BMC Evol. Biol. 11:217.

Yates D., Kittel T., and Cannon R. 2000. Comparing the correlative holdridge model to mechanistic biogeographical models for assessing vegetation distribution response to climatic change. Clim. change 44:59–87.